Proceedings of 16th Int. Workshop on Robotics in Alpe-Adria-Danube Region - RAAD 2007
Ljubljana, June 7-9, 2007

ITERATIVE SOLUTION PARADIGMS FOR UNCALIBRATED VISUAL SERVOING

Mirjana Bonković*
Aleš Hace**
Spomenka Bovan*
Karel Jezernik**

**Faculty of Electrical Engineering, Machine Engineering and Naval Architecture, Split, Croatia*
** *Faculty of Electrical Engineering and Computer Science, Maribor, Slovenia*

Abstract: Uncalibrated, model free, robot visual servoing has been widely applicable in robot vision due to minimal requirements related to calibration and robot kinematic's parameters. The numerical quasi-Newton methods offer a theoretical background for problem solving, which has been proven hard as the real system has been influenced with the noise. Consequently, additional attention has to be paid regarding stability and robustness. In this paper we have presented the simulation results of various, well-known iterative solution efficacy performing the target tracking. Each of the presented approaches originally contributes to numerical method improvement emerging the appropriate paradigm to specific problem solving.

Keywords: Robotics, Visual servoing, Uncalibrated Control, Nonlinear optimization

1. INTRODUCTION

In this paper we have compared the efficacy of various methods for model free uncalibrated visual servoing with fixed imaging. Such systems have been widely applicable in robot vision due to minimal requirements which has to be known related to calibration and robot kinematics' parameters. However, if the robot has been controlled in the unstructured environments, the mentioned problem has been proven hard. Various methods offer specific improvements which are related mostly to the specific task requirements establishing itself as a paradigm for appropriate problem solving. The methods are mostly derived from quasi-Newton approach to the nonlinear problem solving and offer an iterative approach for acquiring an optimal solution. Up to now, there are numerous examples which successfully use described approach for robot visual servoing (Jägersand and Nelson, 1996.), (Piepmeier et al., 2004.), (Shuurman and Capson, 2004.). We have presented the detailed SIMULINK simulation of the methods efficacy performed with four bar planar manipulator.

The rest of the paper is organized as follows. In Section 2 the uncalibrated, model free, image base visual servoing problem is defined with a short review of the standard approaches which can be used for solving the mentioned type of problems. Section 3 describes the appropriate algorithms which result with the specific visual servoing performances obtained during the tracking the defined target along the specific trajectory. In Section 4 we have compared the efficacy of the methods in solving the defined visual tracking problems through the simulations, while Section 5 concludes the paper.

2. PROBLEM FORMULATION

The main goal of the visual servoing is to move the robot tip (or mobile robot) to a certain pose with respect to the particular objects or features in images. Based on the error signal domain, two types of visual servoing system could be defined: image based visual servoing and position based visual servoing (Hutchinson *et al.*, 1996.). The first one assumes that the error is defined in 3D (task space) coordinates, while IBVS is based on the error which is defined in terms of image features. The specification of an image-based visual servo task involves determining an appropriate error function f, such that when the task is achieved, f=0 (Hutchinson *et al.*, 1996.). Visual servoing problem could be formulated as a nonlinear least squares problem in which the goal function F is defined as:

 ISBN 978-961-243-067-2

$$F = \tfrac{1}{2} f(\theta,t)^T f(\theta,t) \tag{1}$$

where f is an appropriate error function, which could be expressed as:

$$\Delta f = J(\theta) * \Delta\theta \tag{2}$$

In (2) $J(\theta)$ is the Jacobian matrix, which relates the rate of change in the image space with the rate of change in the task space.

One of the first and still today very efficient solutions was offered by (Jägersand and Nelson, 1996.) in which he formulated the visual servoing problem as a nonlinear least squares problem solved by a quasi-Newton method using Broyden Jacobian estimation. Stability is ensured using the thrust region method. The similar principles have also been applied for multiple camera model-based 3-D visual servoing (Shuurman and Capson, 2004.).

If the target is moving, the system model has encountered the error not only as a function of robot poses but also of the pose of a moving objects. Consequently, (Piepmeier et al., 2004.) suggests use of the dynamic quasi-Newton with recursive estimation scheme for Jacobian calculation. Recently, the generalized secant method has been proposed (Bonković et al., 2006.) based on the population of iterates which improves the servoing based on the acquired information from past iterates to calibrate at the best the model of a nonlinear function.

In this paper we clearly present the simulation results for uncalibrated vision-guided robotic control and compare the mentioned methods which have usually been used for the similar purpose.

3. THE ALGORITHMS

The visual servoing problem has been formulated as a nonlinear least squares problem (Jägersand and Nelson, 1996.), (Piepmeier et al., 2004.) and it could be solved using quasi-Newton based methods, which consider at each iteration the linear model.

Broyden (Broyden, 1965.) proposed the most successful class of quasi-Newton methods based on the secant equations, imposing the linear model L_{k+1} to exactly match the nonlinear function at iterates x_k and x_{k+1}, that is

$$\begin{aligned} L_{k+1}(x_k) &= F(x_k) \\ L_{k+1}(x_{k+1}) &= F(x_{k+1}) \end{aligned} \tag{3}$$

Subtracting these two equations and defining $y_k = F(x_{k+1}) - F(x_k)$ and $s_k = x_{k+1} - x_k$ we obtain the classical secant equation:

$$B_{k+1} s_k = y_k \tag{4}$$

If the dimension n is strictly greater than 1, there are an infinite number of matrices B_{k+1} satisfying (6). The "least-change secant update", proposed by Broyden, could be desbribed as:

1. minimize $\|B_{k+1} - B_k\|$ (5)
2. use constraint expressed with (4)

which result with the following update formula

$$B_{k+1} = B_k + \lambda s_k^T \tag{6}$$

This method has been proved as successful for visual servoing if an additional technique has been used to improve the robustness and stability of the method. In the rest of this section the various methods have been described which appropriately supplement the quasi-Newton base for nonlinear system solving.

3.1. Reference model

The reference model has been represented based on the real system model described in the Section 4.1. The Jacobian has been determined according to (17). Having in mind the pin-hole camera model, the same relation can be rewritten as:

$$J = J_I J_R = L \cdot \begin{bmatrix} f_x & 0 & -f_x \frac{x_c}{z_c} \\ f_y & 0 & -f_y \frac{y_c}{z_c} \end{bmatrix} \cdot R_C^{rot} \cdot \begin{bmatrix} -\sin(q_1) & -\sin(q_2) \\ \cos(q_1) & \cos(q2) \\ 0 & 0 \end{bmatrix} \tag{7}$$

where L is the robot link length; f_x, f_y are camera internal parameters related with focus length, (x_c, y_c, z_c) are robot tip coordinates, expressed in the camera frame, and q_1, q_2 are actual joints. The R_C^{rot} is the orientation part of the transformation matrix (18). For each iteration, calculated Jacobian (7) serves as a base for control vector calculation.

3.2. Visual servoing by the modified Broyden method

This method has been similar to those described in the introductory part of this section. The pure Broyden method has been sensitive to noise, so numerous authors suggest use of the modified Broyden method, i.e. improved with the factor η (Dodds et al.,), (Donghui et al., 1998). Having this fact in mind, the Jacobian update has been calculated with Broyden estimation according to (8):

$$J_{k+1} = J_k + \eta \frac{\left(y_k - J_k s_k\right) s_k^{\ T}}{s_k^{\ T} s_k} \tag{8}$$

The influence of η has been the subject of our earlier works (Bonković et al., 2006.), while in this paper we reference the method for the efficacy comparison reasons.

3.2. Dynamic visual servoing model

Piepmeier suggests (Piepmeier et al., 2004.) using of the dynamic quasi-Newton with recursive estimation scheme for Jacobian calculation. A new, dynamic visual servoing model has been proposed in which the qualifier "dynamic" refers to the presence of the error velocity term ($\partial f(x_{k+1})/\partial t$). Desired recursive estimation scheme that minimizes a cost function based on the change in the affine model, results with the Jacobian update equation:

$$J_{k+1} = J_k + \frac{\left(y_k - J_k s_k - \frac{\partial f(x_{k+1})}{\partial t} s_t \right) s_k^{\ T}}{\lambda + s_k^{\ T} P_k s_k} \tag{9a}$$

$$P_{k+1} = \frac{1}{\lambda} \left(P_k - \frac{P_k s_k s_k^{\ T} P_k}{\lambda + s_k^{\ T} P_k s_k} \right) \tag{9b}$$

where $y_k = f(x_{k+1}) - f(x_k)$, $s_k = x_{k+1} - x_k$, $s_t = t_{k+1} - t_k$ and $0 < \lambda \le 1$ is a weighting parameter.

3.3. Visual servoing by robot agent action

Jägersand (Jägersand and Nelson, 1996.) studies a robot agent in an unstructured environment. The same problem could also be viewed as the minimization of the functional (1). As a result of the minimization, Jägersand has chosen an unsymmetrical correction term given with the Broyden estimation:

$$J_{k+1} = J_k + \frac{\left(y_k - J_k s_k\right) s_k^{\ T}}{s_k^{\ T} s_k} \tag{10}$$

and the control strategy described in Section 4.2. To maintain the convergence, the thrust region method has been adopted to adjust a parameter α so that the controller never moves out of the validity region of the current Jacobian estimate. To do that, Jägersand solves a constrained problem for $\|\delta_k\| < \alpha$ instead of taking the whole Newton step of a proportional controller:

$$\min_{\|\delta_k\| < \alpha_k} \|y_k - J_k \delta_k\| \tag{11}$$

With the model agreement

$$d_k = \frac{\|J_k \delta_k\|}{\|y_k\|} \tag{12}$$

α has been adjusted according to:

$$\alpha_{k+1} = \begin{cases} \frac{1}{2}\alpha_k & if \quad d_k < d_{lower} \\ \alpha_k & if \quad d_{lower} < d_k \le d_{upper} \\ \max(2\|\delta\|) & if \quad d_k > d_{upper} \end{cases} \tag{13}$$

Consequently, factor α indices the distance for which the estimated model is valid. They have also used a technique known as homotopy methods, which involves the generation of intermediate goals along the way to the main goal y^*. In this paper we have not used the homotopy. Instead, to cope with the noise, we have used the constant η, as (8) indicates, and achieved the improvements using appropriate α.

3.5. Population based uncalibrated visual servoing

Population-based generalization prefer to identify the linear model which is as close as possible to the nonlinear function in the least-squares sense.

At each iteration, the finite population of iterates $x_0....x_{k+1}$ are maintained. The method also belongs to quasi-Newton framework, where B_{k+1} is computed as

$$B_{k+1} = \arg\min_J \left(\sum_{i=0}^{k} \left\| \omega_{k+1}^i F(x_i) - \omega_{k+1}^i L_{k+1}(x_i, J) \right\|_2^2 + \left\| \Gamma J - \Gamma B_{k+1}^0 \right\|_F^2 \right) \tag{14}$$

where L_{k+1} is defined by (3) and the $B_{k+1}^0 \in \Re^{n \times n}$ is an a priori approximation of B_{k+1}. The role of the second term is to overcome the under-determination of the least-square problem based on the first term and also to control the numerical stability of the method. The matrix Γ contains weights associated with the arbitrary term B_{k+1}^0, and the weights $\omega_{k+1}^i \in \Re^+$ are associated with the previous iterates. Equation (14) can be rewritten in matrix form as follows:

$$B_{k+1} = \arg\min_J \left\| J(S_{k+1} I_{n \times m}) \begin{pmatrix} \Omega & 0_{k \times n} \\ 0_{k \times k} & \Gamma \end{pmatrix} - \begin{pmatrix} Y_{k+1} & B_{k+1}^0 \end{pmatrix} \begin{pmatrix} \Omega & 0 \\ 0 & \Gamma \end{pmatrix} \right\|_F^2 \tag{15}$$

where $\Omega \in \Re^{k \times 1}$ is a diagonal matrix with weights ω_{k+1}^i on the diagonal for *i*=0,…,*k*. The normal equations of the least-square problem lead to the following formula:

$$B_{k+1} = B_{k+1}^0 + (Y_{k+1} - B_{k+1}^0 S_{k+1})\Omega^2 S_{k+1}^T (\Gamma^2 + S_{k+1}\Omega^2 S_{k+1}^T)^{-1} \quad (16)$$

where $Y_{k+1} = (y_k, y_{k-1}, ..., y_0)$ and $s_{k+1} = (s_k, s_{k-1}, ..., s_0)$. The role of the a priori matrix B_{k+1}^0 is to overcome the possible under-determination of problem (14). We have chosen $B_{k+1}^0 = B_{k+1}$, which exhibits good properties, so (16) becomes an update formula, which local convergence has been proved in (Crittin and Bierlaire, 2003.). The weights ω_{k+1}^i, capture the relative importance of each iterate in the population, and the matrix Γ captures the importance of the arbitrary terms defined by B_{k+1}^0 for the identification of the linear model. The weights have to be finite and Γ must be such that $\Gamma^2 + S_{k+1}\Omega^2 S_{k+1}^T$ is safely positive definite. To ensure this property we seek for a technique to guarantee both the problem of overcoming the under-determination, and numerical stability. Such problem can be solved in a variety of ways (Crittin and Bierlaire, 2003.), but we have found out that the most appropriate is to define it trough simulations as a small positive constant which guaranties positive definition of the term $\Gamma^2 + S_{k+1}\Omega^2 S_{k+1}^T$.

4. SIMULATION RESULTS

4.1. The system

The simulated system is presented in Figure 1, whereas the simulation scheme is shown in Figure 2. The simulation system consists of the components which characteristics are transformed from real experimental setup applied in our earlier work (Bonković et al., 2006.), which means that during simulations the task has been performed using 2DOF planar parallel manipulator with four revolute joints and a camera that can provide position information of the robot tip and the target in the robot workplace. The robot direct kinematics is given by the following equations,

$$x = L\begin{bmatrix} \cos(q_1) + \cos(q_2) \\ \sin(q_1) + \sin(q_2) \end{bmatrix} \quad (17)$$

where q_1, q_2 are the robot joint angles, and x is a vector of robot tip coordinates in the Cartesian world coordinate frame (Figure 2). *L*=0.4m is the length of the robot single link. Translation and rotation of the camera frame with respect to the robot world base frame is given by the RPY homogenous transformation matrix Rc (18). It is rotated around y-axis for 135°, and translated for 1.2, and 1.2 m in y and z direction respectively.

$$R_C = \begin{bmatrix} 1 & 0 & 0 & 0 \\ 0 & -0.707 & -0.707 & 1.2 \\ 0 & 0.707 & -0.707 & 1.2 \\ 0 & 0 & 0 & 1 \end{bmatrix}. \quad (18)$$

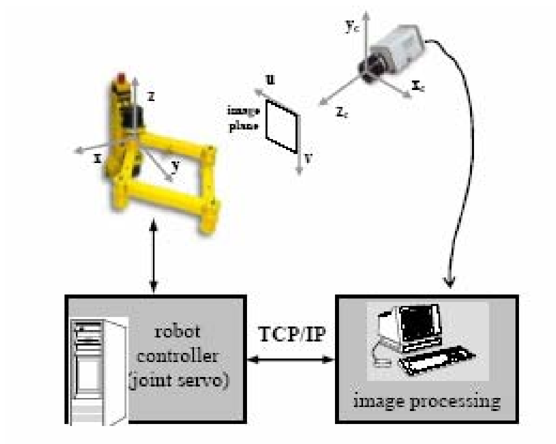

Fig.1. The experimental setup

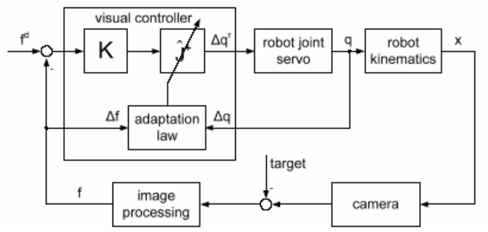

Fig.2. Visual servoing block diagram

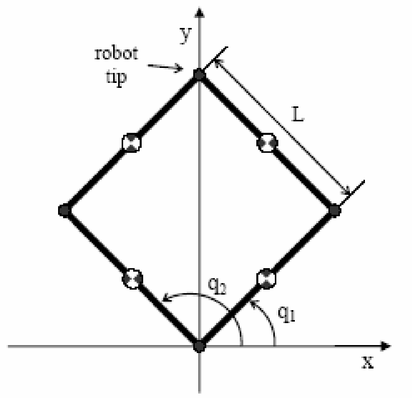

Fig.3. Planar 2DOF parallel manipulator

The block named "robot joint servo" in Figure 1. represents the robot joints dynamics which includes motor, current and velocity-loop. It outputs the position of the robots joints. The velocity closed-loop of the robot joints has been modeled by the first order dynamics:

$$G(s)=100/(s+100) \quad (19)$$

which means that the velocity-loop is very fast with respect to the camera sampling interval (T_{camera}). The input velocity error has been saturated according to robot specification with limit=0.5. The visual feedback gain has been set to K=5.

4.2. The control scheme

In this paper we are interested in robot visual control in a fixed camera configuration. Figure 2 shows the structure of the visual servo system used in this paper. Here, so called image-based visual servoing is considered, in which the error signal that is measured directly in the image, is mapped to the robot actuators' command input. The visual controller is constructed in order to determine the joint velocities $\dot{q}$ as:

$$\dot{q} = J^{+}Ke \tag{20}$$

where J^{+}, K, and e are the pseudoinverse of the Jacobian matrix J that relates joint coordinates with image features, control gain, and the error signal that is obtained by comparing the desired and current image feature parameters, respectively. The robot Jacobian gives relation between robot joint angle velocities and the velocities of its end-effector in Cartesian space. The Jacobian matrix J is a compound of robot and image Jacobian.

$$J = J_I J_R \tag{21}$$

However, the compound Jacobian (21) depends on the system calibration parameters that are hard to obtain accurately in practical applications. In the proposed visual servoing scheme, the Jacobian J is obtained by the estimation process.

4.3. Simulation results

In this paper, the image processing node generates the target point applied in the visual task definition within the image. When the robot tip reached the target, the target point was moved to another position in order to provide traveling of the robot tip through the whole robot work plane. The position of the target point determined corners of the specified "X trajectory" in the image plane. The projection of the target positions on the robot workplane is depicted by Figure 3. The initial robot tip position is marked with "0" and the corresponding robot joint angles have the following values: $q_1 = 30^{\circ}, q_2 = 150^{\circ}$. The initial target position has been the same as the robot tip position, and the consequent positions are marked "1", "2", "3" and "4". The target point positions were generated in the following order: "0"-"1"-"2"-"3"-"4"-"0", and the points have repeated continuously in the specified time interval of 50s.

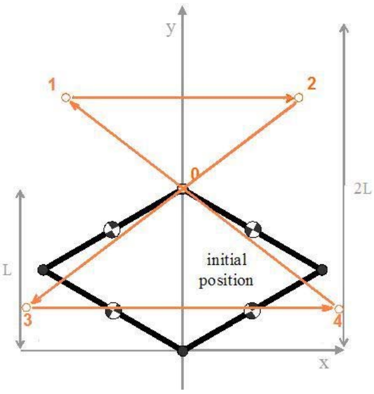

Fig.4. Target movement

For the reference trajectory, marked with points "0"-"1"-"2"-"3"-"4" in Figure 4, the rectangle has been chosen with the upper left corner (-30,57.5) and the down right corner (30,32.5), expressed in the robot base world coordinates. A target has been moving during simulations with constant speed (measured in pixel/s). The trajectory rectangle has the start point T_{start}=(x_end0, y_end0) of the robot tip initial position, X_{max}=*250pixel* and Y_{max}= *200pixel* (in the robot world coordinate base frame) width and height, respectively and T_{camera}=*0.033 s* has been used in simulations as camera refresh rate (measured in s). Simulations have been performed with the sampling time, T_s=0.001s, taking into account that algorithm calculations consumes some amount of time T_{calc}=0.033 s. Along the curves "1"-"2" and "3"-"4" the y component of the speed has been set to zero. The robot tip starts from the point where target is positioned and marked in Figure 4 as "0". It is worth to notice that all simulations have been performed under the geometrical noise of $\pm 0.5\,pixels$, which has been added to the robot tip image position. Also, the robot tip image coordinates have been rounded to integer value, which is a normal procedure related with image data. However, rounding the reference signal also results with noise, which makes the simulations more realistic. We have started our simulations performing the described task using reference robot model. As one can expected, the robot tip traces presented in Figure 5.a., perfectly follows the desired curve. In comparison with the ideal reference model results, the next simulations have been performed with proposed, modified Broyden method, based on the constant η parameter. That method is the simplest variation of a base, Broyden method and results with the worse performance (Figure 5.c.d). Jägersand thrust region methods trades accuracy for time, and it is the slowest method if it is used in combination with homotopy. In this paper, the results have been obtained with thrust region parameters ($d_{lower} = 0.15$ $d_{upper} = 0.27$ $\alpha = 0.92$). The robot tip tracks the trajectory (Figure 5.3.), exposing a visible error, which characterize that the method is not suited for tracking.

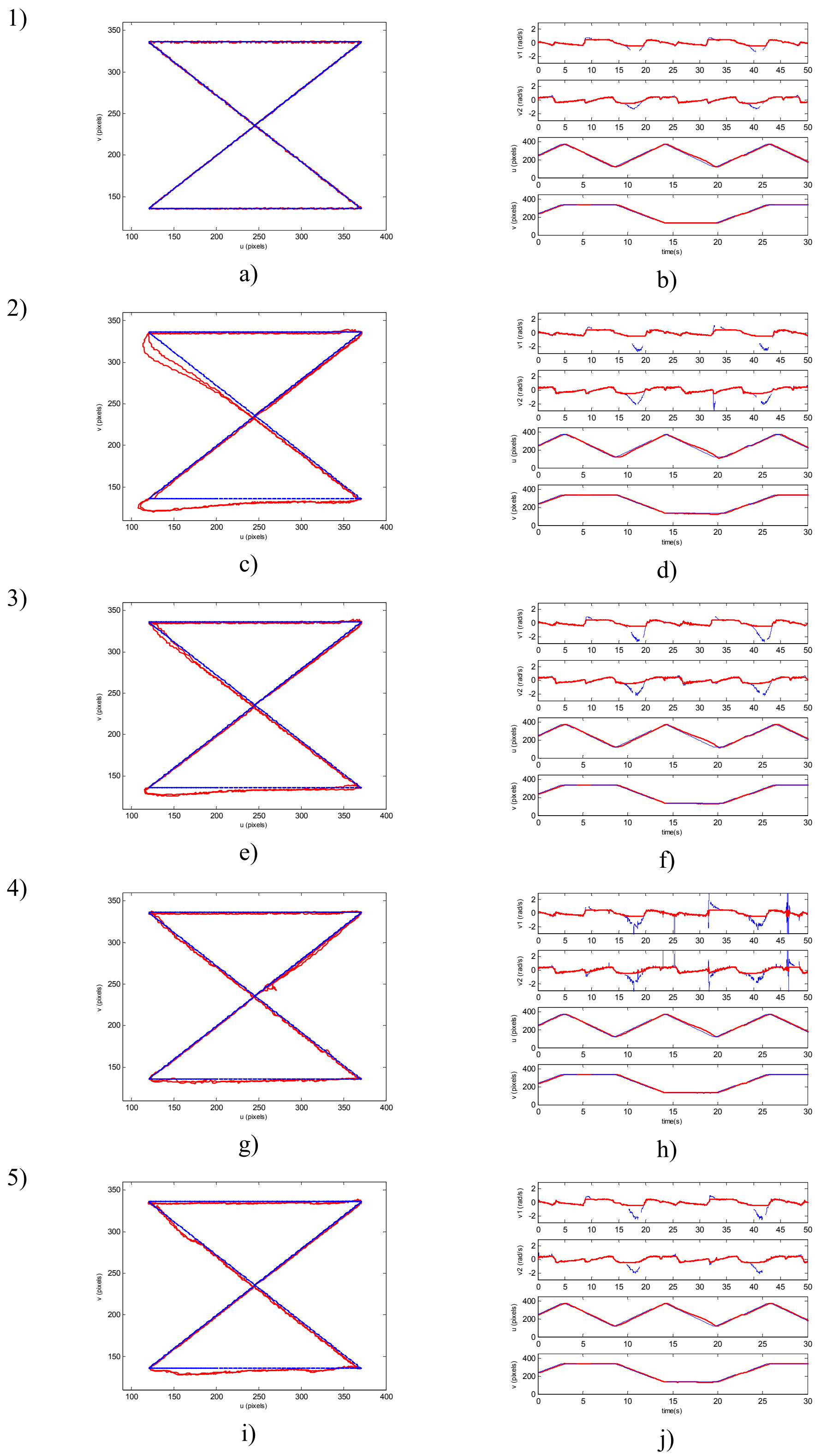

Fig.5. Simulation results - first column: Robot tip trajectory in image coordinates (pixels) for different servoing methods; second column: traces of reference (dashed line) and actual joint speed (solid line);

1) reference model
2) Modified Broyden method with constant η
3) Thrust region method
4) Recursive method introduced by Piepmeier
5) Population based method

Introducing the homotopy procedure, as suggested in (Jägersand and Nelson, 1996.), the method performs very well for static target. The method introduced by Piepmeier, performs very well. We have obtained the results presented in Figure 5.4. for

$$P = \begin{bmatrix} 4 & 0 \\ 0 & 4 \end{bmatrix},$$

and $\lambda = 0.9$. A small suspicion generates the response at the time of 25 s, which may result with unstable behavior if, for example, the noise level introduced in the system becomes bigger. The method has been designed for variable speed target, which we have used in out simulations, so the obtained results have been expected. The last one simulation has been related with the population based method. Even the small deviations can be observed along the trajectory, method results with the best repeatability characteristics. Also, the method is suitable for fast targets, as well as for static target approaching. The traces of the joint's speed have been presented in the Figure 5.b.d.f.h and 5.j., respectively, for each of the mentioned methods. It could be observed that reference speed (dashed-line) has not been reached at the time instances at cca. 19, 24 and 43 sec., which usually corresponds with the trajectory points in which the system Jacobian changes rapidly (corners). As one can see from simulations, each of the methods for uncalibrated visual servoing based on the numerical Jacobian estimation techniques expose the feature which emerge the method as the best choice for a typical task solving, for example: the Piepmeier method is the best for tracking the target which speed varies in time, the Jägersand method is appropriate for static target, the population method offer a good repeatability under static and dynamic target approaching, while Broyden method performs the best under no noise condition.

5. CONCLUSION

The problem of visual servoing in unstructured environments, without using any a-priori camera or kinematic models has proven hard. Unfortunately, there are many such environments where robots would be useful. In this paper we compare the efficiency of the methods which have been proved as successful in performing a typical trajectory following task. Although all methods have been declared as quasi-Newton based, simulation shows that additional attention have to be paid in overwhelming the unwanted system characteristics. Consequently, appropriate method's improvement yields the uncalibrated visual servoing paradigm which offers the solution for typical task solving. Piepmeier offers the integral solution for moving target tracking in which two advances have to be taken into consideration: dynamic update which takes into account the target speed and the recursive solution which is the noise resistant. Population based approach has been proven as a numerical method which performances are superior over the similar quasi-Newton methods. It is also suitable for noise environment and it can be supplemented with dynamical update from Piepmeir. Jägersand use classical Broyden update with thrust region to improve the stability. Although the thrust region trades the accuracy for speed, Jägersand's results have been experimentally confirmed as very succesfull. The intention of the paper is to enable the clear simulation expose of the typical methods performance obtained through typical uncalibrated servoing trajectory tracking which could serve as a good base which helps in choosing the appropriate method for the specific task solving.

REFERENCES

Bonković M., Hace A., Jezernik K., ”A new method for uncalibrated visual servoing”, Proc. of AMC, Istanbul, Turkey, pp.624-629., 2006.

Broyden C.G., "A class of methods for solving nonlinear simultaneous equations", Mathematics of Computation 19, pp. 577-593, 1965.

Crittin F., Bierlaire M., “A generalization of secant methods for solving nonlinear systems of equations”, in Proc. 3rd Swiss Transport Research Conference, March 19-21, 2003.

Dodds G., Zatari A.* and Bischof R., “Uncalibrated Visual Servoing for Full Motion Dextrous Robot Systems with Tracking Cameras” (http://robotik.w3.rz.unibw-muenchen.de/PDF/UnViSer.pdf)

Donghui Li, Jinping Zeng, Shuzi Zhou. “Convergence of Broyden-Like Matrix”, Appl. Math. Lett. Vol. 11, No. 5, pp.35-37, 1998, Elsevier Science, Ltd.

Hutchinson S., Hager G. D., Corke P., “A Tutorial on Visual Servo Control”, IEEE Trans. On Robotics and Automation, Vol.12, No.5, Oct 1996.

Jägersand M., Nelson R., “On-line Estimation of Visual-Motor Models using Active Vision”, Proc. ARPA Image Understanding Workshop 1996.

Piepmeier J. A., McMurray G. V., Lipkin H. “Uncalibrated Dynamic Visual Servoing”, IEEE Trans. On Robotics and Automation, Vol.20, No.1, pp. 143-147, February 2004.

Shuurman D.C., Capson D.W., “Robust Direct Visual Servo Using Network-Synchronized Cameras”, Trans. On Robotics and Automation, pp. 319-334Vol.20, No.2, Apr. 2004.